Polímeros
ISSN 1678-5169 (Online)

https://doi.org/10.1590/0104-1428.20250013

ORIGINAL ARTICLES

Characterization of PBAT bioplastic with Brazil nut urchin particles

Bruno Mello de Freitas[1,2]*, Carlos do Amaral Razzino[3] and Paulo Noronha Lisboa Filho[2]

[1]Departamento de Engenharia de Materiais, Laboratório de Materiais – LabMat, Universidade do Estado do Amazonas – UEA, Manaus, AM, Brasil

[2]Departamento de Física e Meteorologia, Faculdade de Ciências, Universidade Estadual Paulista – UNESP, Bauru, SP, Brasil

[3]Departamento de Engenharia de Produção, Faculdade de Engenharia, Universidade Estadual Paulista – UNESP, Bauru, SP, Brasil

**bm.freitas@unesp.br*

Abstract

This study developed PBAT (poly[butylene adipate-co-terephthalate]) biocomposites with 10 wt% and 20 wt% Brazil nut urchin particles by extrusion and injection. TGA showed thermal stability up to 275°C (10 wt%) and 250°C (20 wt%), with degradation peaks near 400°C. XRD indicated maintained crystallinity, with the 10 wt% composite having the highest peak intensity (5254 a.u.). FTIR confirmed molecular interactions through characteristic OH (3442 cm^{-1}) and C=O (1710-1720 cm^{-1}) peaks. SEM revealed better surface integrity at 10 wt%, while 20 wt% showed porosity and poor adhesion. Tensile strength decreased from 9.36 MPa (PBAT) to 7.08 MPa (10 wt%) and 6.7 MPa (20 wt%). Elongation reduced, whereas Young's modulus increased to 210 MPa (10 wt%) and 316 MPa (20 wt%). Shore D hardness improved by over 40%, but impact resistance dropped by up to 88%. These biocomposites show potential for applications requiring higher stiffness and hardness, contributing to sustainable plastic alternatives.

Keywords: *composite materials, forest residues, biopolymers, PBAT, Brazil nut urchin.*

Data Availability: Research data is available upon request from the corresponding author.

How to cite: Freitas, B. M., Razzino, C. A., & Lisboa Filho, P. N. (2025). Characterization of PBAT bioplastic with Brazil nut urchin particles. *Polímeros: Ciência e Tecnologia*, *35*(4), e20250048. https://doi.org/10.1590/0104-1428.20250013

1. Introduction

As production processes improve, waste reduction methods are also advancing, focusing on better resource use, recycling, energy efficiency, and lowering environmental impact[1]. In recent years, polymer materials have progressed significantly due to concerns about environmental damage from the exacerbated consumption of oil reserves[2,3]. While petroleum-based plastics are widely used in packaging and construction[4,5], they pose serious environmental challenges because of the non-degradable waste they produce[6].

Plastics play an important role in sustainability by being lightweight, improving fuel efficiency in vehicles, and extending food shelf life to reduce waste. However, environmental concerns about plastic waste and greenhouse gas emissions are accelerating the shift towards a circular plastics economy. In this model, the use of non-renewable resources and waste generation is minimized, with focus on reuse and recycling throughout the material life cycle[7].

Most commercial plastics are made from fossil resources, but they can also be produced from renewable sources, known as bioplastics[7]. Bioplastics are defined as plastics that are biobased, biodegradable, produced through biological processes, or a combination of these. Some biodegradable plastics made from fossil fuels are also considered bioplastics[8].

PBAT (Poly [Butylene Adipate Co-Terephthalate]) is a widely used and promising biodegradable polymer that can replace non-biodegradable plastics[9]. It consists of terephthalic acid, adipic acid, and 1,4-butanediol, with biodegradability attributed to the butylene adipate group[10] and can replace polyethylene (PE), which is not biodegradable. PBAT has similar flexibility to PET and is suitable for industrial applications thanks to its high elongation and good processability[11]. Similarly, increasing terephthalate content or molecular weight boosts stiffness and tensile strength but reduces elongation[9]. However, the use of PBAT remains commercially limited, although it could be enhanced by adding Brazil nut urchin residue.

The Brazil nut urchin (Bertholletia excelsa H&B Lecythidaceae) is a lignocellulosic organic agricultural waste and also a source of carbon, especially for the production of "green" composite materials. The accumulation of this waste leads to an increase in environmental pollution, and the accidental deposition of this waste in landfills can affect the permeability of rainwater in the soil. However, although material waste is inevitable, agro-industrial waste in the form of fibers, husks, shells, powders, particles, etc., can be recycled and reused in innovative ways in various sectors[12].

Thus, these materials form cheap "new or secondary resources", which make them more valuable and more widely usable.

Major efforts around the world are seeking to address the problem of single-use plastics and the ecological damage they cause[13]. It is estimated that 4.8-12.7 million tons of plastic can enter marine ecosystems every year[14]. However, to date, few studies have been reported on how Brazil nut urchin particles can improve the performance of PBAT biopolymer through extrusion and injection processing. Therefore, this work analyzed the effects on the mechanical and thermal properties of PBAT biopolymer after the addition of Brazil nut urchin waste particles in the proportion of 10 wt% and 20 wt% through the extrusion and injection process as a sustainable and ecological alternative.

2. Materials and Methods

2.1 Materials

After the Brazil nut seeds were removed, the Brazil nut urchins were harvested at the Aruanã farm, linked to the company ECONUT - a pioneering company in Brazil nut plantations, in Itacoatiara, a municipality located 270 km from the capital Manaus, in the state of Amazonas, Brazil. The urchins were stored in a rain-protected warehouse for about a week after they were harvested, ensuring that they didn't get damp.

The polymer matrix in the form of pellets and of the PBAT type with a maximum thickness of 0.061 mm was purchased from the company Tiken LTDA. The main characteristics of PBAT are: density of 1.21 g/cm^3; melting point of 116 ~ 122°C; vicat A/50 ≥ 80°C; tensile strength ≥ 25 MPa; Elongation ≥ 400%; and moisture ≤ 0.06%.

2.2 Methods

The Brazil nut urchin was broken by hammering, resulting in smaller, irregular pieces. After breaking, they were washed with running water to remove impurities from the forest. Finally, the pieces were dried in a QUIMIS model Q317M-72 oven at a temperature of 70 ± 2°C for 12 hours. The urchins were then ground in a MARCONI knife mill and classified by sieve size in a PROSUTEST vibrator for approximately 25 minutes. The particles that passed through the 40 mesh sieve, equivalent to an opening of 0.35 mm, were selected and dried together with the PBAT pellets in a QUIMIS oven at a temperature of 70 ± 2°C for 12 hours. After drying, the urchin particles and PBAT were aggregated in a plastic bag by manual stirring in proportions of 10 wt% and 20 wt% of the urchin.

The selection of 10% and 20% wt ratios was based on commonly used ranges for natural fiber biocomposites (5–30% wt), allowing evaluation of mechanical, thermal, and morphological effects without compromising extrusion or causing excessive agglomeration. These intermediate ratios are thus suitable for exploratory and comparative studies.

With the mixture aggregated, the extrusion process was carried out using a hopper fed by a single-screw extruder with a useful screw length / external screw diameter = 40, model ZGH 28950. The temperature used was 138°C to 149°C between the 4 stages of operation. The extruded biocomposites were then cooled in a water bath, pelletized in a BGM grinder, model BGM.2, series 0002.25, and dried in an oven at a temperature of 70 ± 2°C for 12 hours to remove the moisture and make the plastic injection samples.

Plastic injection of the test specimens was carried out in a HAITIAN injection molding, model HTF60W-II, with a feed temperature of 189 ± 2°C and a homogenization temperature of 215 ± 5°C. The standard used was ASTM D412 for the tensile, impact and hardness tests.

In order to perform a brittle fracture on the biocomposites after the injection process, a sample of each material was immersed in a Styrofoam container with liquid nitrogen for 10 seconds, then removed and gently fractured with tweezers so that there was as little effort as possible. This technique was used to evaluate the interaction between PBAT and the nut urchin using scanning electron microscopy (SEM). The equipment used for SEM was a Carl Zeiss model EVO-LS15. The samples were fixed to stubs with carbon tape, used in high vacuum mode at an accelerating voltage of 5 kV and coated twice with gold. The behavior of the biocomposites after extrusion was also analyzed in SEM.

To determine the thermal stability and degradation temperatures of the constituents, the TGA and DTG techniques were used a Jupiter STA 449 F3 thermal analyzer (NETZSCH) on 30 mg of the samples using a 150 µL open α-alumina crucible. The temperature conditions ranged from 30 to 700°C with a heating rate of 10°C.min^{-1}, in a dynamic dry air flow atmosphere with a flow rate of 50 mL min^{-1}. The MiniFlex 6th generation RIGAKU X-ray diffractometer (XRD) was used to analyze the crystal structure of the materials with a Cu Kα radiation source (λ= 1.5418 Å), 40 kV, 15 mA, continuous flow, divergence slit: 1/4°, scan mode: 2θ, Range: 10° to 90°, step size: 0.04° time per step: 3.00 s and ω: 1.5°. FTIR analysis, used to effectively study the molecular interactions that occur during reactive extrusion, was carried out on a BRUKER spectrophotometer with the attenuated total reflection (ATR). The absorption spectra were obtained from 32 scans per sample with a resolution of 4 cm^{-1}. The frequency performed was between 400 and 4000 cm^{-1}.

The mechanical properties of all the samples were determined by tensile, impact and shore D hardness tests, with 5 samples (CP's) in each test. The tensile test was carried out on an EMC universal testing machine with a 30 kN load cell and a test speed of 5 mm/min. The tensile test followed the ASTM D638 standard, type III with specimen length of 165 mm, reduced section of 57 mm, gauge width of 13 mm, overall width of 19 mm and thickness of 3 mm. The impact resistance test was carried out in accordance with ASTM D256 on a TINIUS OLSEN model 892, with the thickness and width of the samples being approximately 3 and 14 mm, respectively. The Shore D hardness test was carried out on a portable digital INSTRUTHERM device, model DP-400.

3. Results and Discussions

3.1 Thermogravimetry (TG / DTG)

Figure 1 shows the analysis of the TG tests and their DTG derivative for all the samples. Although the Brazil

nut urchin sample was dried, there is an obvious loss of mass up to 100°C, due to the elimination of water and the urchin's hydrophilic characteristics, and for PBAT and the biocomposites this does not occur to such an extent. For the urchin there is an exothermic loss of mass between 210 and 345°C (from 90 to 40%) which can be attributed to the decomposition of hemicellulose and cellulose, with maximum degradation temperatures at 285 and 325°C, respectively. Lignin degradation occurs between 350 and 540°C[15]. Table 1 lists the results of the TG analysis in detail for the biomasses found in the Brazil nut urchin.

The thermal degradation (TG) results show that PBAT and the 10 wt% biocomposite remain stable up to 275°C, while the 20 wt% biocomposite degrades from 250°C. The degradation of PBAT and biocomposites began at approximately 300°C and ended at 520°C, with the peak degradation occurring near 400°C. The first degradation stage (340–400°C) is likely due to the decomposition of aliphatic copolyester components (adipic acid and 1,4-butanediol), while the second stage (~600°C) corresponds to the decomposition of the aromatic terephthalic copolyester[16]. This increase in thermal resistance can be attributed to the hydrophobic characteristics of the PBAT present in the composite.

The DTG analysis shows three degradation stages. The urchin partially degrades with peaks at 280°C and 320°C, while the main degradation peaks occur at 395°C for PBAT, 405°C for the 10 wt% biocomposite, and 400°C for the 20 wt% biocomposite. At 535°C there is ash residue for the biocomposites and PBAT, and in the urchin this temperature increased to 555°C, due to the presence of lignin[17]. The PBAT visibly inhibited the degradation of the hemicellulose and cellulose of the urchin between 210 and 345°C.

3.2 X-Ray Diffraction (XRD)

The natural fibers of the Brazil nut urchin consist mainly of cellulose (both amorphous and crystalline), along with hemicellulose and lignin (amorphous)[2,18]. Since PBAT is semi-crystalline[3], adding urchin fibers is expected to modify the composite's crystallinity. Table 2[19] compares PBAT's crystallographic planes with research results, showing similarities.

XRD shows that the crystallinity of PBAT was not compromised by the addition of urchin particles (Figure 2). The 10 wt% biocomposite had the highest peak intensity (5254 a.u. at 22.88°), followed by the 20 wt% biocomposite (3428 a.u. at 23.12°) and the urchin (3207 a.u. at 22.32°).

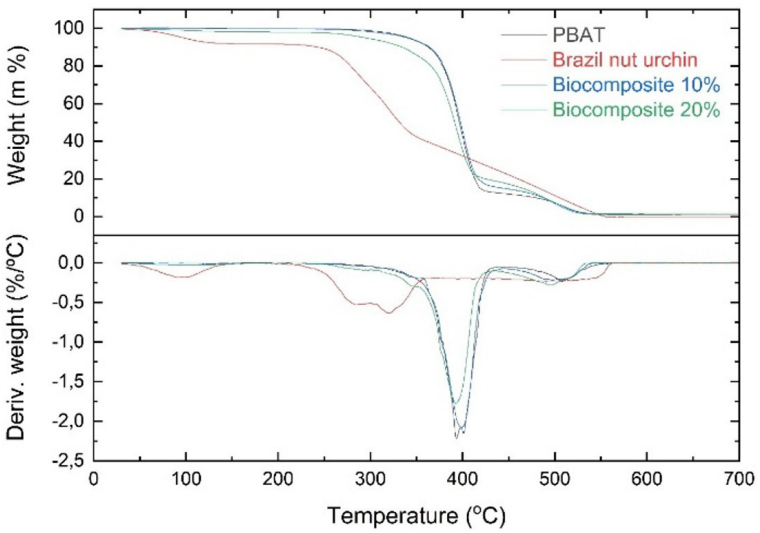

Figure 1. TG and DTG of PBAT samples, Brazil nut urchin and biocomposites with 10 wt% and 20 wt% of urchin.

Table 1. TG results of biomass components for Brazil nut urchin.

Sample	Moisture Release	Hemicellulose	Cellulose	Lignin	Solid Residue
	T Range (°C)	T Range (°C)	T Range (°C)	T Range (°C)	T (°C)
Brazil nut urchin	50-140	210-285	285-345	350-540	555

Table 2. XRD plane data of PBAT and 10 wt% and 20 wt% biocomposites.

d_{hkl}	(0$\bar{1}$1)	(010)	($\bar{1}$02)	(100)	($\bar{1}$11)	($\bar{1}\bar{1}$2, 012, 101)	(1$\bar{2}$1, 1$\bar{2}$0, 120)
2θ[19]	16.00°	17.22°	20.12°	23.00°	24.72°	28.52°	30.95°
2θ	16.08°	17.36°	20.04°	22.80°	24.76°	28.88°	30.92°

Source: [19]adapted by the author.

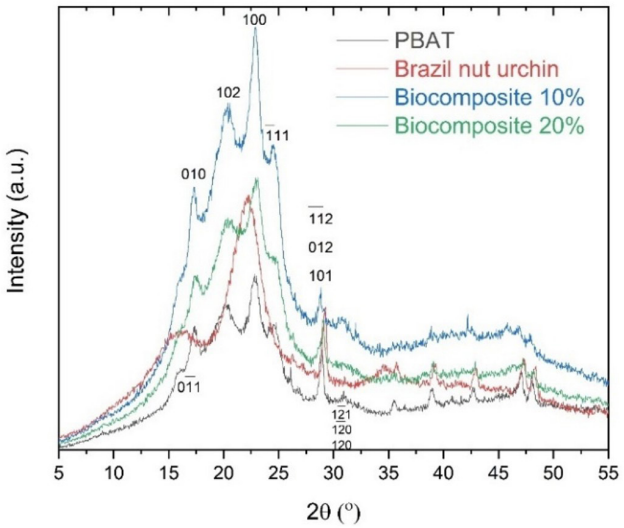

Figure 2. XRD of PBAT, urchin and biocomposites with 10 wt% and 20 wt% of Brazil nut urchin.

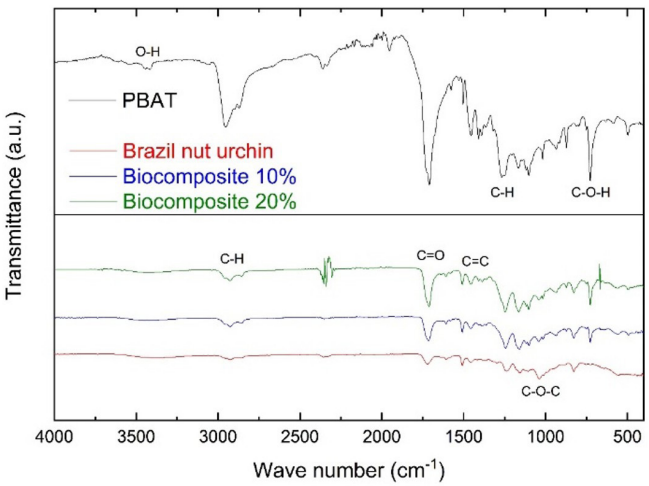

Figure 3. FTIR: PBAT, urchin, biocomposite with 10 wt% and 20 wt% of Brazil nut urchin.

Lower lignin contents acted as nucleating agents, increasing crystallinity, but high contents restricted the organization of the PBAT polymer chains, resulting in a reduction in total crystallinity[17]. The peak height was not directly proportional to the addition of urchin.

3.3 Fourier transform infrared spectroscopy (FTIR)

FTIR analysis helps study molecular interactions during reactive extrusion[20] and identifies fiber functional groups[21]. Key absorption peaks are expected at 2900–3600 cm^{-1} for cellulose (-OH/CH), 1700–1770 cm^{-1} for hemicellulose (C=O), and 1200–1600 cm^{-1} for lignin (methoxy-O-CH_3/C-O-C/C=C)[22].

Figure 3 shows a weak absorbance peak at 3511 cm^{-1} in biocomposites, attributed to OH stretching[23]. The peak at 3442 cm^{-1}, characteristic of PBAT, corresponds to a weak OH stretching band associated with the vibrations of the hydroxyl linked to the hydrogen (-OH) in the starch chains[24], also appears in biocomposites but with lower intensity. Spectral changes indicate interactions between PBAT and urchin particles. FTIR spectra show peaks at 2925-2952 cm^{-1} from CH_2 aliphatic C-H stretching[16]. The FTIR spectra also show the presence of lignin in the PBAT matrix due to the appearance of the CH stretching vibration peak. A sharp peak, between 1710 and 1720 cm^{-1}, represents the carbonyl groups of carboxylic, p-coumaric, ferulic and uronic acid, which are the main constituents of extractives and hemicellulose[25], and another peak at 1708 cm^{-1} attributed to the ester carbonyl stretch (C=O) of the ester group, which was originally present in the PBAT structure[16,26]. A reduction in the C=O peak signals polymer degradation[16]. Biocomposites show C=C phenylene stretching peaks at 1456 and 1508 cm^{-1}, while PBAT has them at 1409 and 1454 cm^{-1}[18].

The peaks between 1236 and 1267 cm^{-1} are attributed to C-H deformation (asymmetric), representing the crystalline nature and vibration of CH_2 in cellulose[27], and for PBAT it is attributed to C-O stretching of the ester bonds[16]. The peaks at 1037-1162 cm^{-1} correspond to C-O-C stretching in cellulose glycosidic bonds[28-30]. The sharp peak at 727 cm^{-1} is linked to -CH_2- vibrations in the PBAT structure[16].

Table 3 shows that peak frequencies remain similar despite adding urchin to the bioplastic. If a compatibilizer had been used, a greater intensity of these peaks would have been evident[20]. According to the harmonic oscillator model, peak frequency decreases with stronger molecular interactions, where hydrogen bonds play a key role[31].

3.4 Microscopia eletrônica de varredura (SEM)

As the Brazil nut urchin content increased, the surfaces of the biocomposites became rougher (Figure 4). The biocomposite with 10 wt% by weight of urchin showed better structural integrity and a smoother, denser appearance (Figure 4b), while the 20 wt% biocomposite was more irregular, with ripples, depressions, and pores (Figure 4d). These findings align with Pan et al.[19] who observed increased surface irregularity with higher fiber content. These results highlight the importance of mechanical and barrier properties in nanocomposite films[20], indicating weak interfacial adhesion with the matrix, corroborating the FTIR results. The urchin was homogeneously dispersed in the polymer matrix and present across the biocomposite surface, though some pores were observed (Figure 4d). This differences in dispersion were likely due to extrusion processing, which is more effective than gravity and press processing, but still resulted in irregular fractures and visible cracks (Figure 4).

Figure 5 highlights poor compatibility between the polymer matrix and the urchin surface. This may be due to the different surface energies, which prevent the formation of a stable and well-adhered interface, causing defects and porosity. This lack of interfacial adhesion can negatively impact the composite's mechanical properties[32]. Chemical treatment removes surface impurities from the fiber, enhancing mechanical interlocking with the matrix and improving the composite's mechanical properties[33]. Figure 5 also shows

Table 3. XRD plane data of PBAT and 10 wt% and 20 wt% biocomposites.

Sample (cm^{-1})	O-H	C-H	C=O	C=C	C-H	C-O-C	C-O-H
PBAT	3500	2952	1708	1454 / 1409	1267	1103	727
Urchin	3442	2925	1720	-	1236	1037	-
Bio 10 wt%	3442	2925	1716	1456 / 1508	1245	1161	727
Bio 20 wt%	3442	2925	1710	1456 / 1508	1245	1162	727

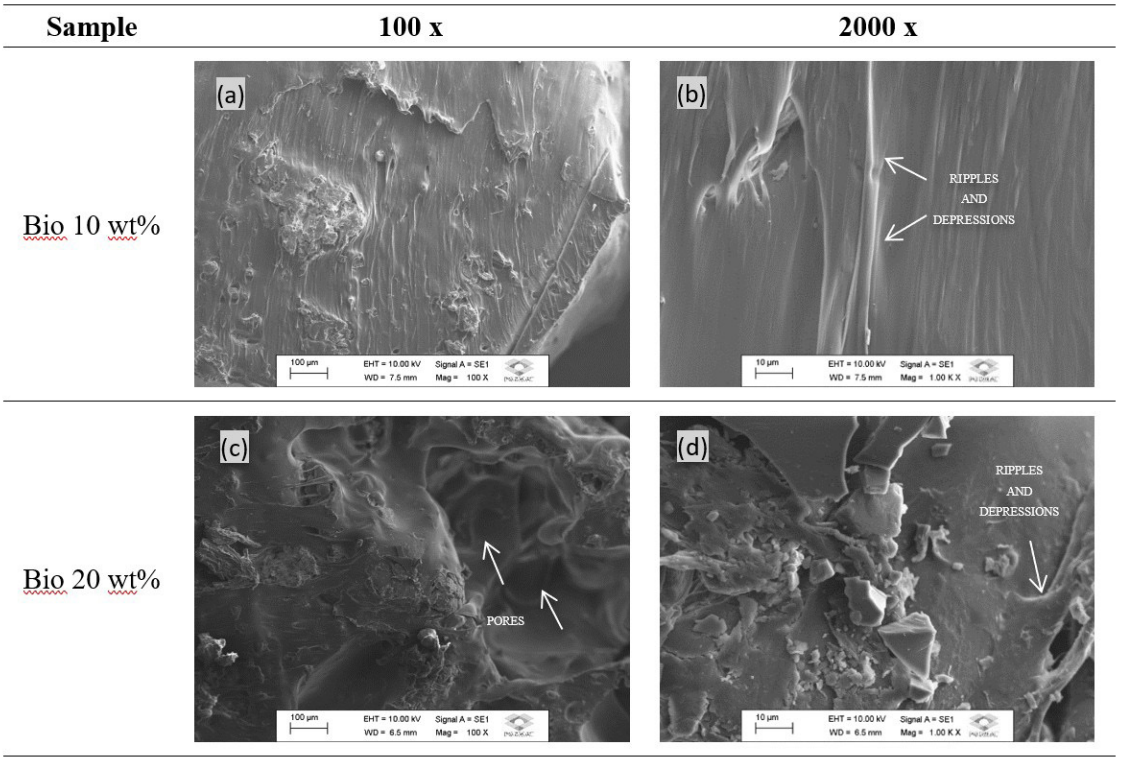

Figure 4. SEM after extrusion of (a) and (b) biocomposite with 10 wt% (c) and (d) biocomposite with 20 wt% of Brazil nut urchin.

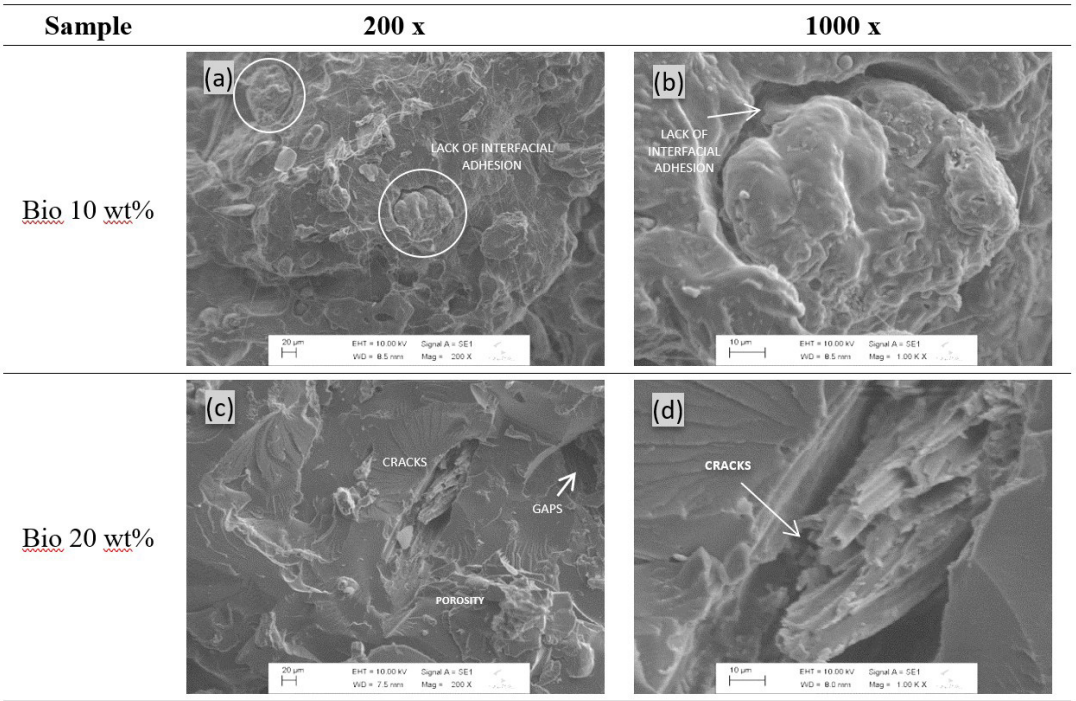

Figure 5. SEM after fracturing with liquid nitrogen of (a) and (b) biocomposite with 10 wt%; (c) and (d) biocomposite with 20 wt% of Brazil nut urchin.

poor distribution and orientation of urchin fibers in the polymer matrix, likely due to the extrusion process, though better than gravity and pressing methods, however the surface showed irregular and visible fractures or cracks, which indicates the typical fragility of lignocellulosic materials[20]. The inadequate distribution, fiber agglomeration and gaps suggest processing issues related to temperature, pressure, and cooling rate. Reprocessing the biocomposite through extrusion could help mitigate these problems.

3.5 Mechanical tests

3.5.1 Tensile test

The addition of urchin reduced the tensile stress (σ) of PBAT from 9.36 MPa to 7.08 MPa (10 wt% urchin) and 6.7 MPa (20 wt% urchin). This aligns with previous studies showing reduced PBAT tensile strength when reinforced with materials like starch[20], cellulose nanocrystals[34], cellulose acetate[35], ground coffee[36], organomontmorillonite[37] and wheat straw[38]. The 10 wt% biocomposite had stress comparable to low-density polyethylene (LDPE, 6.9-16 MPa) but significantly lower than polyesteramide (PEA, 17 MPa), polypropylene (PP, 35 MPa), and linear LDPE, which are commonly used in packaging and agriculture[39].

Figure 6b shows that adding urchin significantly reduced elongation: from 24.23% in pure PBAT to 10.85% with 10 wt% urchin, and 5.89% with 20 wt%, indicating a decrease in the material's plastic deformation under tension. Figure 6c shows that the elastic modulus (Young's modulus) increased with urchin content - from 131 MPa in pure PBAT to 210 MPa (10 wt%) and 316 MPa (20 wt%). This rise is likely due to phase transition[20] good lignin dispersion, and strong PBAT-lignin interactions[40]. In addition, there are also hydrogen bonds and π-π interactions[41], as lignin has a rigid aromatic structure and a high Young's modulus[42].

3.5.2 Izod impact test

The highest impact resistance was observed in pure PBAT (206.44 J/m), while the addition of 10 wt% and 20 wt% urchin reduced it to 47.37 J/m and 32.67 J/m, respectively - an 88.38% decrease (Figure 7). This indicates that urchin makes the biocomposite more fragile, consistent with tensile test results showing increased stiffness and reduced plastic deformation.

Composite materials are highly sensitive to impact, which can cause severe internal damage like delamination and cracking[43]. Composites with a polypropylene (PP) matrix and long natural fibers show the highest impact resistance, likely due to better interfacial stress transfer. It was also found that the treatment of the fibers with a coupling agent (maleic anhydride) reduces the loss of impact resistance[44].

Literature reports a Charpy impact energy of 115 kJ/m^2 for flax fiber PP composites manufactured by the pultrusion process[45], and for a compression molded an Izod impact of 751 J/m for needle-punched flax blankets[46], a value 14x higher than that found in the biocomposite with 10 wt% of nut urchin. For bioplastics, PLA reinforced with 30 wt% Cordenka fiber achieved the highest biodegradable composite impact strength at 72 kJ/m^2[47]. Additionally, PLA composites with 30 wt% abaca and synthetic cellulose fibers showed significant improvements in Charpy impact strength and tensile strength (5.7 to 7.9 kJ/m^2)[48].

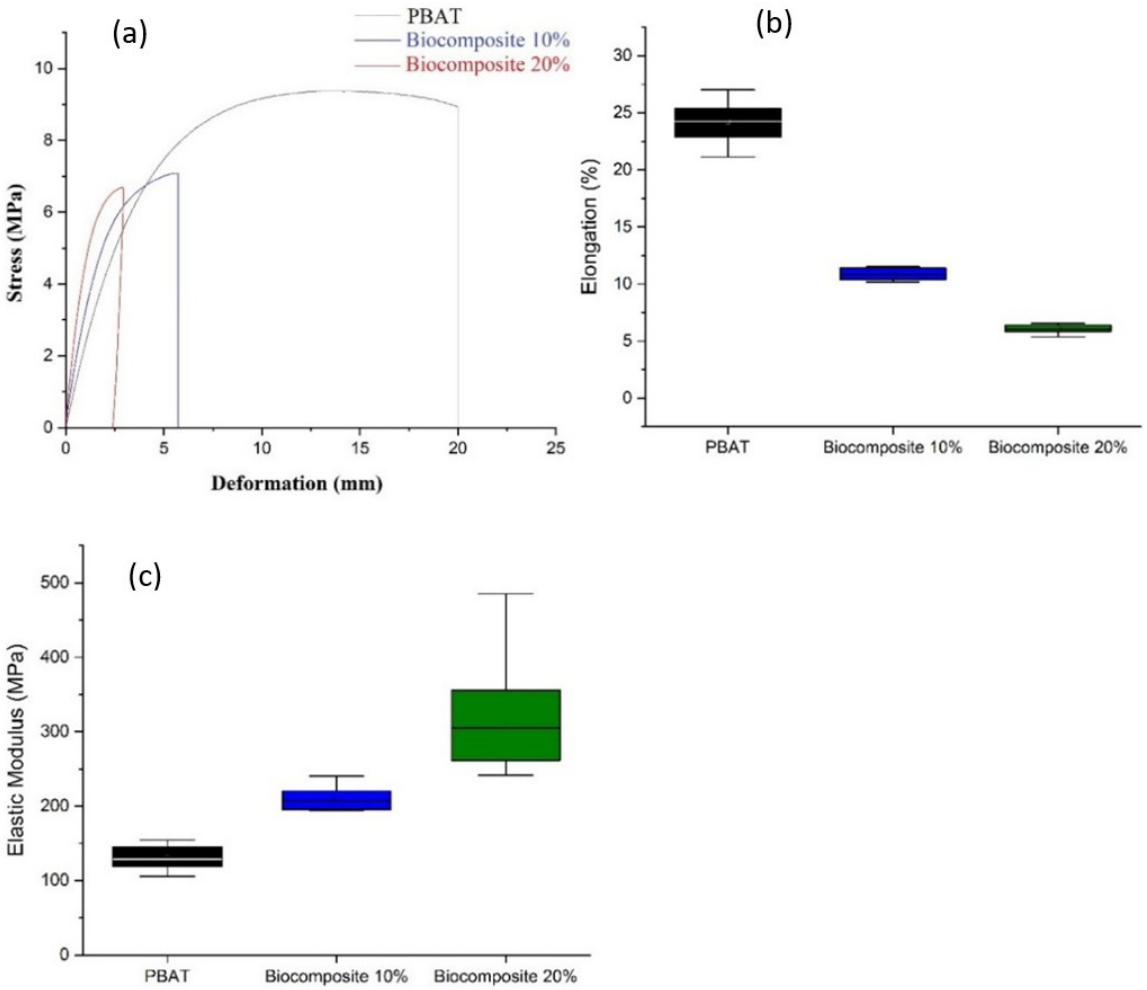

Figure 6. Curves (a) Stress-deformation; (b) Elongation; (c) Elastic modulus.

3.5.3 Shore D surface hardness test

The surface hardness (Shore D) of PBAT biocomposites increased with the addition of Brazil nut urchin particles, possibly due to the greater stiffness and hardness of the fibers compared to the PBAT matrix. At the proportion of 20 wt% the biocomposite showed over 30% higher average surface hardness, with an increase of more than 40% from 28.3 (PBAT) to 39.7 Shore D (Figure 8). Another aspect analyzed in the interquartile range was that a higher amount of urchin particles allowed for more efficient load distribution, resulting in a surface more resistant to penetration and, consequently, increased surface hardness (Figure 8).

Despite some compatibility limitations observed under microscopy, the fiber presence still enhanced hardness. With 10 wt% urchin, the hardness was lower compared to 20 wt%, but it still led to a higher hardness than pure PBAT, resulting in an intermediate value of 35 Shore D. The lower fiber content also added strength to PBAT, which showed a lower surface hardness (29 Shore D) due to its natural flexibility and reduced stiffness compared to reinforced materials (Figure 8).

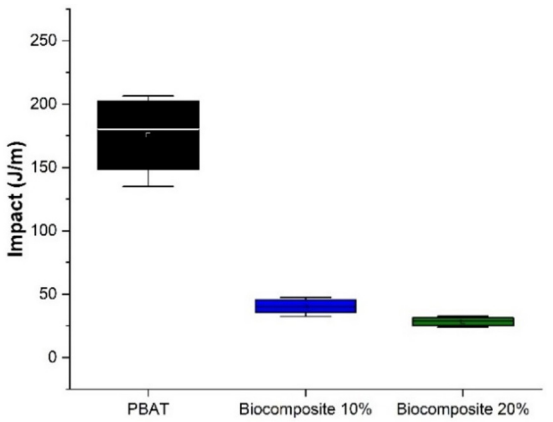

Figure 7. Izod impact strength for PBAT and biocomposites with 10 wt% and 20 wt% of Brazil nut urchin.

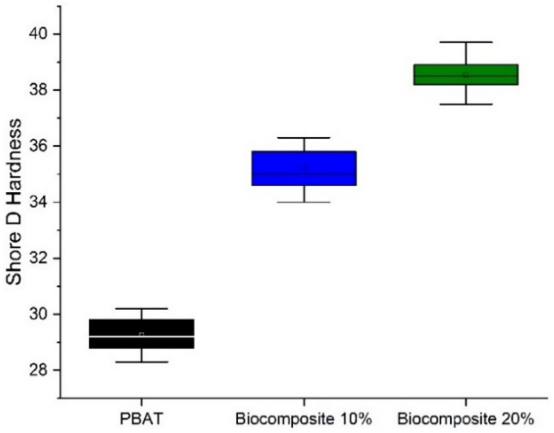

Figure 8. Shore D surface hardness resistance for PBAT and biocomposite with 10 wt% and 20 wt% of Brazil nut urchin.

4. Conclusions

After processing, all biocomposite samples showed good surface homogeneity and were classified as particulate polymer biocomposites. While biocomposites begin degrading around 300°C, urchin particles degrade from 210°C, slightly lowering the ash degradation onset for PBAT with 20 wt% urchin to 493°C. XRD analysis showed no significant change in crystallinity after extrusion. However, SEM revealed poor interfacial adhesion between PBAT and natural fibers, weakening the composite's mechanical properties. The mechanical properties results suggest that the urchin acted as a filler rather than a reinforcement, due to the decrease in PBAT's tensile strength, toughness and ductility, making them more brittle than pure PBAT, mainly due to weak particle-matrix bonding and morphological pores. On the other hand, higher fiber content improved surface hardness due to the rigidity of the urchin fibers, making the material more suitable for high-hardness applications. Because natural fiber composites are lighter than those with synthetic fibers, they offer energy savings in sectors like automotive. Thus, PBAT/urchin composites show advantages for industrial applications, helping reduce plastic use, environmental impact, and supporting the circular economy.

5. Author's Contribution

- **Conceptualization** – Bruno Mello de Freitas; Paulo Noronha Lisboa Filho.
- **Data curation** – Bruno Mello de Freitas.
- **Formal analysis** – Bruno Mello de Freitas.
- **Funding acquisition -** Carlos do Amaral Razzino; Paulo Noronha Lisboa Filho.
- **Investigation** – Bruno Mello de Freitas.
- **Methodology** – Bruno Mello de Freitas; Paulo Noronha Lisboa Filho.
- **Project administration** – Bruno Mello de Freitas; Paulo Noronha Lisboa Filho.
- **Resources** – Paulo Noronha Lisboa Filho.
- **Software** – NA.
- **Supervision** – Bruno Mello de Freitas; Paulo Noronha Lisboa Filho.
- **Validation** – Bruno Mello de Freitas; Carlos do Amaral Razzino; Paulo Noronha Lisboa Filho.
- **Visualization** – Bruno Mello de Freitas.
- **Writing – original draft** – Bruno Mello de Freitas.
- **Writing – review & editing** – Carlos do Amaral Razzino; Paulo Noronha Lisboa Filho.

6. Acknowledgements

The authors acknowledge the Fundação de Amparo à Pesquisa do Estado do Amazonas-FAPEAM, Universidade Estadual Paulista "Júlio de Mesquita Filho"-UNESP, Universidade do Estado do Amazonas-UEA, Laboratório de Materiais-LabMat and Grupo de Física Aplicada à Medicina e Nanotecnologia-GFAMN, Avanplas Polímeros da Amazônia, ECONUT, Brasil.

7. References

1. Nandy, S., Fortunato, E., & Martins, R. (2022). Green economy and waste management: an inevitable plan for materials science. *Progress in Natural Science*, *32*(1), 1-9. https://doi.org/10.1016/j.pnsc.2022.01.001.
2. Chen, J., Long, Z., Wang, S., Meng, Y., Zhang, G., & Nie, S. (2019). Biodegradable blends of graphene quantum dots and thermoplastic starch with solid-state photoluminescent and conductive properties. *International Journal of Biological Macromolecules*, *139*, 367-376. https://doi.org/10.1016/j.ijbiomac.2019.07.211. PMid:31377295.
3. Wu, Z., Huang, Y., Xiao, L., Lin, D., Yang, Y., Wang, H., Yang, Y., Wu, D., Chen, H., Zhang, Q., Qin, W., & Pu, S. (2019). Physical properties and structural characterization of starch/polyvinyl alcohol/graphene oxide composite films. *International Journal of Biological Macromolecules*, *123*, 569-575. https://doi.org/10.1016/j.ijbiomac.2018.11.071. PMid:30439436.
4. Tian, H., Wang, K., Liu, D., Yan, J., Xiang, A., & Rajulu, A. V. (2017). Enhanced mechanical and thermal properties of poly (vinyl alcohol)/corn starch blends by nanoclay intercalation. *International Journal of Biological Macromolecules*, *101*, 314-320. https://doi.org/10.1016/j.ijbiomac.2017.03.111. PMid:28341175.
5. Wang, S., Ren, J., Li, W., Sun, R., & Liu, S. (2014). Properties of polyvinyl alcohol/xylan composite films with citric acid. *Carbohydrate Polymers*, *103*, 94-99. https://doi.org/10.1016/j.carbpol.2013.12.030. PMid:24528705.
6. Ferreira, F. V., Pinheiro, I. F., Gouveia, R. F., Thim, G. P., & Lona, L. M. F. (2018). Functionalized cellulose nanocrystals as reinforcement in biodegradable polymer nanocomposites. *Polymer Composites*, *39*(S1), E9-E29. https://doi.org/10.1002/pc.24583.
7. Rosenboom, J.-G., Langer, R., & Traverso, G. (2022). Bioplastics for a circular economy. *Nature Reviews. Materials*, *7*(2), 117-137. https://doi.org/10.1038/s41578-021-00407-8. PMid:35075395.
8. Karan, H., Funk, C., Grabert, M., Oey, M., & Hankamer, B. (2019). Green bioplastics as part of a circular bioeconomy. *Trends in Plant Science*, *24*(3), 237-249. https://doi.org/10.1016/j.tplants.2018.11.010. PMid:30612789.
9. Kanwal, A., Zhang, M., Sharaf, F., & Li, C. (2022). Polymer pollution and its solutions with special emphasis on Poly (butylene adipate terephthalate (PBAT)). *Polymer Bulletin*, *79*(11), 9303-9330. https://doi.org/10.1007/s00289-021-04065-2.

10. Elvers, D., Song, C. H., Steinbüchel, A., & Leker, J. (2016). Technology trends in biodegradable polymers: evidence from patent analysis. *Polymer Reviews (Philadelphia, Pa.)*, *56*(4), 584-606. https://doi.org/10.1080/15583724.2015.1125918.
11. De Hoe, G. X., Zumstein, M. T., Getzinger, G. J., Rüegsegger, I., Kohler, H.-P. E., Maurer-Jones, M. A., Sander, M., Hillmyer, M. A., & McNeill, K. (2019). Photochemical transformation of poly (butylene adipate-co-terephthalate) and its effects on enzymatic hydrolyzability. *Environmental Science & Technology*, *53*(5), 2472-2481. https://doi.org/10.1021/acs.est.8b06458. PMid:30726677.
12. Das, O., Babu, K., Shanmugam, V., Sykam, K., Tebyetekerwa, M., Neisiany, R. E., Försth, M., Sas, G., Gonzalez-Libreros, J., Capezza, A. J., Hedenqvist, M. S., Berto, F., & Ramakrishna, S. (2022). Natural and industrial wastes for sustainable and renewable polymer composites. *Renewable & Sustainable Energy Reviews*, *158*, 112054. https://doi.org/10.1016/j.rser.2021.112054.
13. Miller, S. A. (2020). Five misperceptions surrounding the environmental impacts of single-use plastic. *Environmental Science & Technology*, *54*(22), 14143-14151. https://doi.org/10.1021/acs.est.0c05295. PMid:33103887.
14. Jambeck, J. R., Geyer, R., Wilcox, C., Siegler, T. R., Perryman, M., Andrady, A., Narayan, R., & Law, K. L. (2015). Plastic waste inputs from land into the ocean. *Science*, *347*(6223), 768-771. https://doi.org/10.1126/science.1260352. PMid:25678662.
15. Apaydın Varol, E., & Mutlu, Ü. (2023). TGA-FTIR analysis of biomass samples based on the thermal decomposition behavior of hemicellulose, cellulose, and lignin. *Energies*, *16*(9), 3674. https://doi.org/10.3390/en16093674.
16. Zehetmeyer, G., Meira, S. M. M., Scheibel, J. M., Oliveira, R. V. B., Brandelli, A., & Soares, R. M. D. (2016). Influence of melt processing on biodegradable nisin-PBAT films intended for active food packaging applications. *Journal of Applied Polymer Science*, *133*(13), 43212. https://doi.org/10.1002/app.43212.
17. Kargarzadeh, H., Galeski, A., & Pawlak, A. (2020). PBAT green composites: effects of kraft lignin particles on the morphological, thermal, crystalline, macro and micromechanical properties. *Polymer*, *203*, 122748. https://doi.org/10.1016/j.polymer.2020.122748.
18. Tavares, L. B., Ito, N. M., Salvadori, M. C., Santos, D. J., & Rosa, D. S. (2018). PBAT/kraft lignin blend in flexible laminated food packaging: peeling resistance and thermal degradability. *Polymer Testing*, *67*, 169-176. https://doi.org/10.1016/j.polymertesting.2018.03.004.
19. Pan, H., Ju, D., Zhao, Y., Wang, Z., Yang, H., Zhang, H., & Dong, L. (2016). Mechanical properties, hydrophobic properties and thermal stability of the biodegradable poly (butylene adipate-co-terephthalate)/maleated thermoplastic starch blown films. *Fibers and Polymers*, *17*(10), 1540-1549. https://doi.org/10.1007/s12221-016-6379-x.
20. Zhai, X., Wang, W., Zhang, H., Dai, Y., Dong, H., & Hou, H. (2020). Effects of high starch content on the physicochemical properties of starch/PBAT nanocomposite films prepared by extrusion blowing. *Carbohydrate Polymers*, *239*, 116231. https://doi.org/10.1016/j.carbpol.2020.116231. PMid:32414453.
21. Caban, R. (2022). FTIR-ATR spectroscopic, thermal and microstructural studies on polypropylene-glass fiber composites. *Journal of Molecular Structure*, *1264*, 133181. https://doi.org/10.1016/j.molstruc.2022.133181.
22. Kamarudin, S. H., Rayung, M., Abu, F., Ahmad, S., Fadil, F., Abdul Karim, A., Norizan, M. N., Sarifuddin, N., Mat Desa, M. S. Z., Mohd Basri, M. S., Samsudin, H., & Abdullah, L. C. (2022). A review on antimicrobial packaging from biodegradable polymer composites. *Polymers*, *14*(1), 174. https://doi.org/10.3390/polym14010174. PMid:35012197.
23. Katakojwala, R., & Mohan, S. V. (2020). Microcrystalline cellulose production from sugarcane bagasse: sustainable process development and life cycle assessment. *Journal of Cleaner Production*, *249*, 119342. https://doi.org/10.1016/j.jclepro.2019.119342.
24. Zuo, Y., Gu, J., Yang, L., Qiao, Z., Tan, H., & Zhang, Y. (2013). Synthesis and characterization of maleic anhydride esterified corn starch by the dry method. *International Journal of Biological Macromolecules*, *62*, 241-247. https://doi.org/10.1016/j.ijbiomac.2013.08.032. PMid:23999015.
25. Sain, M., & Panthapulakkal, S. (2006). Bioprocess preparation of wheat straw fibers and their characterization. *Industrial Crops and Products*, *23*(1), 1-8. https://doi.org/10.1016/j.indcrop.2005.01.006.
26. Wei, D., Wang, H., Xiao, H., Zheng, A., & Yang, Y. (2015). Morphology and mechanical properties of poly (butylene adipate-co-terephthalate)/potato starch blends in the presence of synthesized reactive compatibilizer or modified poly (butylene adipate-co-terephthalate). *Carbohydrate Polymers*, *123*, 275-282. https://doi.org/10.1016/j.carbpol.2015.01.058. PMid:25843859.
27. Huang, M.-F., Yu, J.-G., & Ma, X.-F. (2004). Studies on the properties of montmorillonite-reinforced thermoplastic starch composites. *Polymer*, *45*(20), 7017-7023. https://doi.org/10.1016/j.polymer.2004.07.068.
28. Sun, X. F., Xu, F. Q., Sun, R. C., Geng, Z. C., Fowler, P., & Baird, M. S. (2005). Characteristics of degraded hemicellulosic polymers obtained from steam exploded wheat straw. *Carbohydrate Polymers*, *60*(1), 15-26. https://doi.org/10.1016/j.carbpol.2004.11.012.
29. Garcia, P. S., Grossmann, M. V. E., Shirai, M. A., Lazaretti, M. M., Yamashita, F., Muller, C. M. O., & Mali, S. (2014). Improving action of citric acid as compatibiliser in starch/polyester blown films. *Industrial Crops and Products*, *52*, 305-312. https://doi.org/10.1016/j.indcrop.2013.11.001.
30. Pawlak, A., & Mucha, M. (2003). Thermogravimetric and FTIR studies of chitosan blends. *Thermochimica Acta*, *396*(1-2), 153-166. https://doi.org/10.1016/S0040-6031(02)00523-3.
31. Wang, F., Sun, X., Zan, J., Li, M., Liu, Y., & Chen, J. (2022). Terahertz spectra and weak intermolecular interactions of nucleosides or nucleoside drugs. *Spectrochimica Acta. Part A, Molecular and Biomolecular Spectroscopy*, *265*, 120344. https://doi.org/10.1016/j.saa.2021.120344. PMid:34481145.
32. Wang, H., Liu, X., Liu, J., Wu, M., & Huang, Y. (2022). Tailoring interfacial adhesion between PBAT matrix and PTFE-modified microcrystalline cellulose additive for advanced composites. *Polymers*, *14*(10), 1973. https://doi.org/10.3390/polym14101973. PMid:35631855.
33. Verma, D., & Goh, K. L. (2021). Effect of mercerization/alkali surface treatment of natural fibres and their utilization in polymer composites: mechanical and morphological studies. *Journal of Composites Science*, *5*(7), 175. https://doi.org/10.3390/jcs5070175.
34. Pinheiro, I. F., Ferreira, F. V., Souza, D. H. S., Gouveia, R. F., Lona, L. M. F., Morales, A. R., & Mei, L. H. I. (2017). Mechanical, rheological and degradation properties of PBAT nanocomposites reinforced by functionalized cellulose nanocrystals. *European Polymer Journal*, *97*, 356-365. https://doi.org/10.1016/j.eurpolymj.2017.10.026.
35. Wu, C.-S. (2012). Characterization of cellulose acetate-reinforced aliphatic–aromatic copolyester composites. *Carbohydrate Polymers*, *87*(2), 1249-1256. https://doi.org/10.1016/j.carbpol.2011.09.009. PMid:23399153.
36. Moustafa, H., Guizani, C., Dupont, C., Martin, V., Jeguirim, M., & Dufresne, A. (2017). Utilization of torrefied coffee grounds as reinforcing agent to produce high-quality biodegradable PBAT composites for food packaging applications. *ACS Sustainable Chemistry & Engineering*, *5*(2), 1906-1916. https://doi.org/10.1021/acssuschemeng.6b02633.

37. Li, J., Lai, L., Wu, L., Severtson, S. J., & Wang, W.-J. (2018). Enhancement of water vapor barrier properties of biodegradable poly (butylene adipate-co-terephthalate) films with highly oriented organomontmorillonite. *ACS Sustainable Chemistry & Engineering*, *6*(5), 6654-6662. https://doi.org/10.1021/acssuschemeng.8b00430.
38. Le Digabel, F., & Avérous, L. (2006). Effects of lignin content on the properties of lignocellulose-based biocomposites. *Carbohydrate Polymers*, *66*(4), 537-545. https://doi.org/10.1016/j.carbpol.2006.04.023.
39. Guimarães, M., Jr., Botaro, V. R., Novack, K. M., Teixeira, F. G., & Tonoli, G. H. D. (2015). High moisture strength of cassava starch/polyvinyl alcohol-compatible blends for the packaging and agricultural sectors. *Journal of Polymer Research*, *22*(10), 192. https://doi.org/10.1007/s10965-015-0834-z.
40. Sugano-Segura, A. T. R., Tavares, L. B., Rizzi, J. G. F., Rosa, D. S., Salvadori, M. C., & Santos, D. J. (2017). Mechanical and thermal properties of electron beam-irradiated polypropylene reinforced with Kraft lignin. *Radiation Physics and Chemistry*, *139*, 5-10. https://doi.org/10.1016/j.radphyschem.2017.05.016.
41. Morelli, C. L., Belgacem, M. N., Branciforti, M. C., Bretas, R. E. S., Crisci, A., & Bras, J. (2016). Supramolecular aromatic interactions to enhance biodegradable film properties through incorporation of functionalized cellulose nanocrystals. *Composites. Part A, Applied Science and Manufacturing*, *83*, 80-88. https://doi.org/10.1016/j.compositesa.2015.10.038.
42. Elder, T. (2007). Quantum Chemical Determination of Young's Modulus of Lignin. Calculations on a β− O-4 'Model Compound. *Biomacromolecules*, *8*(11), 3619-3627. https://doi.org/10.1021/bm700663y. PMid:17927244.
43. Shah, S. Z. H., Karuppanan, S., Megat-Yusoff, P. S. M., & Sajid, Z. (2019). Impact resistance and damage tolerance of fiber reinforced composites: A review. *Composite Structures*, *217*, 100-121. https://doi.org/10.1016/j.compstruct.2019.03.021.
44. Pickering, K. L., Efendy, M. A., & Le, T. M. (2016). A review of recent developments in natural fibre composites and their mechanical performance. *Composites. Part A, Applied Science and Manufacturing*, *83*, 98-112. https://doi.org/10.1016/j.compositesa.2015.08.038.
45. Angelov, I., Wiedmer, S., Evstatiev, M., Friedrich, K., & Mennig, G. (2007). Pultrusion of a flax/polypropylene yarn. *Composites. Part A, Applied Science and Manufacturing*, *38*(5), 1431-1438. https://doi.org/10.1016/j.compositesa.2006.01.024.
46. Oksman, K. (2000). Mechanical properties of natural fibre mat reinforced thermoplastic. *Applied Composite Materials*, *7*(5), 403-414. https://doi.org/10.1023/A:1026546426764.
47. Bax, B., & Müssig, J. (2008). Impact and tensile properties of PLA/Cordenka and PLA/flax composites. *Composites Science and Technology*, *68*(7-8), 1601-1607. https://doi.org/10.1016/j.compscitech.2008.01.004.
48. Bledzki, A. K., Jaszkiewicz, A., & Scherzer, D. (2009). Mechanical properties of PLA composites with man-made cellulose and abaca fibres. *Composites. Part A, Applied Science and Manufacturing*, *40*(4), 404-412. https://doi.org/10.1016/j.compositesa.2009.01.002.

Received: May 10, 2025
Revised: Aug. 13, 2025
Accepted: Sep. 24, 2025

Associate Editor: *José A. C. G. Covas*